PREDICTION OF THERMODYNAMIC PROPERTIES OF Al_2O_3–SiO_2 SYSTEM MELTS

I.A. GONCHAROV[1], **V.I. GALINICH**[1], **D.D. MISHCHENKO**[1] and **V.S. SUDAVTSOVA**[2]
[1]E.O. Paton Electric Welding Institute, NASU
11 Bozhenko Str., 03680, Kiev, Ukraine. E-mail: office@paton.kiev.ua
[2]I.M. Frantsevich Institute of Problems of Materials Science, NASU
3 Krzhizhanovsky Str., 03680, Kiev, Ukraine

Aluminium and silicon oxides are included into the composition of fluxes for welding, electroslag remelting and metallurgical slags. Knowledge of thermodynamic properties of aluminium oxide–silicon oxide system mixtures will allow evaluation of the nature of their interaction in the melt that will provide an insight into the metallurgical properties of the respective materials for welding and related technologies developed on their base. Analysis of published data on phase equilibria of constitutional diagrams of aluminium oxide–silicon oxide system and thermodynamic properties of this system was performed. It is established that the constitutional diagram data are correct, and experimental values of activities of these melt components are characterized by large scatter. The coordinates of liquidus line of the constitutional diagram of aluminium oxide–silicon oxide system were used to calculate the thermodynamic activities of aluminium oxide at its concentration in the range of 0.7–1.0. It is established that they start manifesting small negative deviations from ideal solutions in the eutectic melt (0.74). Integration of Gibbs–Dugem equation was performed to assess the activities of silicon oxide. It was determined that they demonstrate slight negative deviations from ideal solutions. It is shown that the influence of aluminium oxide–silicon oxide system melts on the nature of interaction in complex multicomponent solutions can be significant. It is found that addition of thermodynamically stable chemical compounds (for instance, sillimanite) to multicomponent slag melts leads to lowering of their oxidizing ability. Replacement of quartz sand and alumina by disthen-sillimanite concentrate in agglomerated flux charge leads to lowering of thermodynamic activity of oxygen in the slag melt, slows down running of silicon-reduction process and reduces manganese losses in welding. 25 Ref., 6 Figures.

Keywords: *aluminium and silicon oxides, constitutional diagrams, thermodynamic activity of components, slag melts, fluxes for welding and electroslag remelting*

Aluminium and silicon oxides are included into the fluxes for welding, electroslag remelting and metallurgical slags [1]. In multicomponent slag melts on their base, complex alumosiliconoxygen anions of different degrees of polymerization form, which determine the melt physico-chemical properties, and technological and metallurgical properties of the respective materials, accordingly. Knowledge of thermodynamic properties of Al_2O_3–SiO_2 system melts is required to predict the thermodynamic properties of the respective ternary and quaternary slag systems, which include binary Al_2O_3–SiO_2 system, and improvement of currently available welding fluxes and metallurgical slags.

In this connection, the objective of this work was analysis of the available published data on phase equilibria and thermodynamic properties of Al_2O_3–SiO_2 system mixtures, as well as calculation of activity of components of liquid solutions, proceeding from the coordinates of liquidus line in a broad concentration range.

The first publication of phase diagram [2] is in agreement with the data on liquidus line coordinates [3]. The authors showed that $3Al_2O_3{\cdot}2SiO_2$ compound called mullite [4] is more stable in air at atmospheric pressure than sillimanite (Al_2SiO_5). Experimental data on phase equilibria in this system were determined more precisely and were analyzed, for instance, in [5–15].

In [5, 6] different factors influencing mullite melting were also considered, and in [12] the invariant compositions and their temperatures were summed up. All these data and some of the more recent ones are given in Figure 1, from which it is easy to visualize the modern constitutional diagram of Al_2O_3–SiO_2 system.

SiO_2 eutectic — mullite, according to the data of [13], has the following coordinates: 1545 °C; 3.3 mol.% Al_2O_3, that is confirmed by thermal data [14], according to which the average eutectic temperature is 1546 °C.

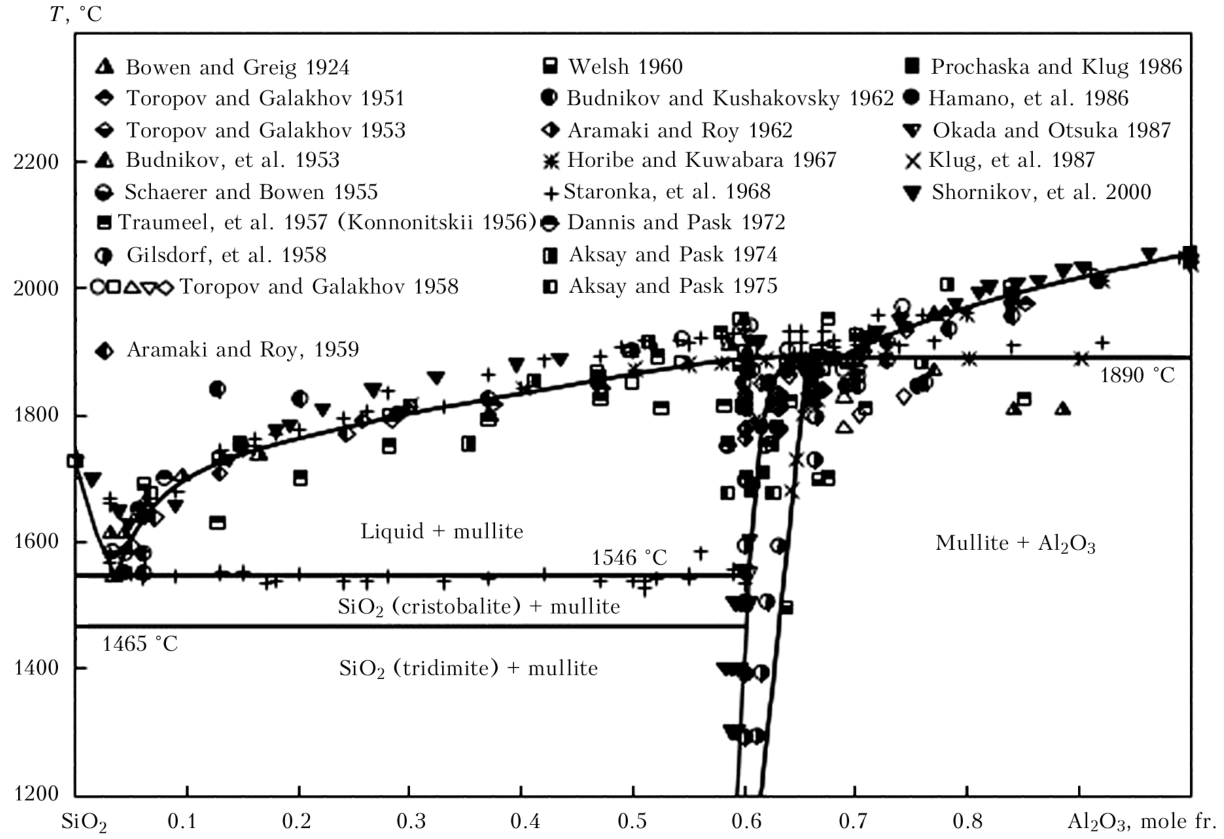

Figure 1. Constitutional diagram of Al_2O_3–SiO_2 system by the data of different authors

Considering the data given in Figure 1, we can come to the conclusion that mullite (65.3 mol.% Al_2O_3) melts in a congruent manner at 1891.5 °C, and mullite–Al_2O_3 eutectic contains 68.5 mol.% Al_2O_3 and melts at 1890 °C. It is also found that mullite decomposes at $T < 434$ °C.

A. Zajtsev with co-authors [16] studied the activities of silicon oxide in mullite–Al_2O_3 two-phase region at 1200 and 1480 °C by the method of Knudsen effusion mass-spectrometry (KEMS), using pure SiO_2 as a standard condition. Ignoring the temperature impact, it was found that activity $a_{Al_2O_3} = 0.56$.

S. Shornikov with co-authors [17] applied the same method to study partial pressures of different particles over the mullite solution and obtained $a_{Al_2O_3} = 0.37$ at 1550 and 0.18 between 1660 and 1760 °C.

In [18] differential KEMS method was used to determine $a_{Al_2O_3}$ in melts of Al_2O_3–SiO_2 system at 1600 and 1700, 1800 °C with ±20 % error. Considering that the initial samples were non-equilibrium, and had high viscosity, this prevented establishment of equilibrium during the experiments. In view of the above, these results cannot be regarded as valid. Moreover, the determined $a_{Al_2O_3}$ demonstrate very large negative deviations from the Raoult law that is uncharacteristic for systems with weak interparticle interaction, to which the considered system belongs.

KEMS method was used to study the activities of silicon dioxide in this system melts at 1927, 2027 and 2127 °C [19]. From Figure 2 it is seen that $a_{Al_2O_3}$ values derived in [19] have alternating deviations from ideal solutions and slight temperature dependence.

The same method was used in [20] to determine $a_{Al_2O_3}$ at 1748 and 1877 °C in melts of Al_2O_3 with SiO_2 up to aluminium oxide concentration ≤0.6. These data demonstrate the smallest negative deviations from Raoult law.

In [21] KEMS method was used to determine $a_{Al_2O_3}$ in a broader compositional range at 1577 and 1677 °C. It is found that in the region of SiO_2-enriched liquid solutions, $a_{Al_2O_3}$ activity demonstrates slight negative, and at $a_{Al_2O_3} > 0.3$ – positive deviations from Raoult law. At penetration into the heterogeneous region at $a_{Al_2O_3} > 0.6$, SiO_2 activities, as was anticipated, acquire constant values.

Modelling $a_{Al_2O_3}$ of the system mixtures in the entire compositional range was performed in works [22, 23] using a package of applied software Thermocalc and Factsage, respectively. SiO_2 activities determined in these works, are given in Figure 2. It is clear that they correlate

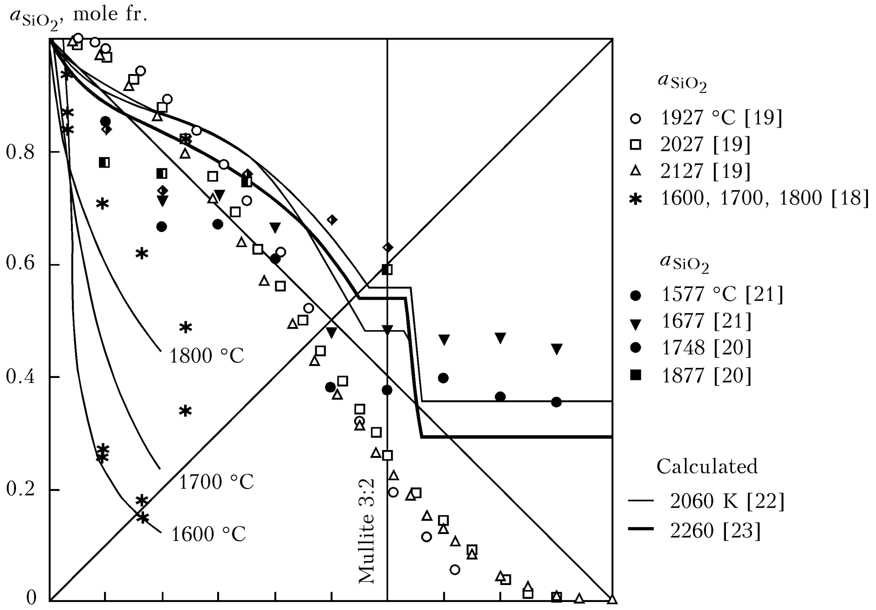

Figure 2. Activities of Al_2O_3–SiO_2 system melt components

with the data from one of the more recent studies [21].

Considering the great scatter of data in experimentally established $a_{Al_2O_3}$ (see Figure 2), we calculated $a_{Al_2O_3}$ from the liquidus line coordinates in composition region of $0.7 < x_{Al_2O_3} < 1$ by the procedure developed by us [24]. It turned out that $a_{Al_2O_3}$ demonstrate values, close to ideal solutions. This is not surprising, as the properties of Al_2O_3 and SiO_2 are similar and, therefore, the energies of their interaction, either in solid, or in liquid state, cannot be strong. Moreover, we find that in eutectic melt $a_{Al_2O_3}$ activity starts manifesting slight negative deviations from ideal solutions. Considering that they will remain just as small with increase of SiO_2 content, we have extrapolated them to the entire composition region (Figure 3).

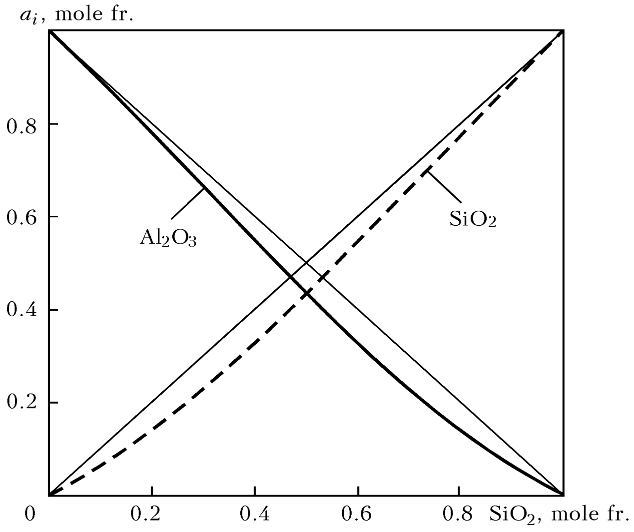

Figure 3. Activities of Al_2O_3–SiO_2 system melt components calculated from liquidus line coordinates at 2160 K

From the thus obtained $a_{Al_2O_3}$, the $a_{Al_2O_3}$ values were calculated by integration of Gibbs–Dugem equation (Figure 3). As was anticipated, $a_{Al_2O_3}$ also demonstrate slight negative deviations from ideal solutions, i.e. reveal a similar dependence.

All the known experimental results on activities of Al_2O_3–SiO_2 system melt components are characterized by large errors, which due to that, first, the studied alloys often were non-equilibrium, secondly, all of them are had very high viscosity, because of which the alloy composition can change during high-temperature investigations, in connection with predominant evaporation of one of the components. Therefore, the experiments should be followed by chemical analysis of the samples, and then the obtained results would be more adequate.

Alloys of this system cannot demonstrate large negative deviations from ideal solutions, as it was obtained in [18]. Results of [17] are not

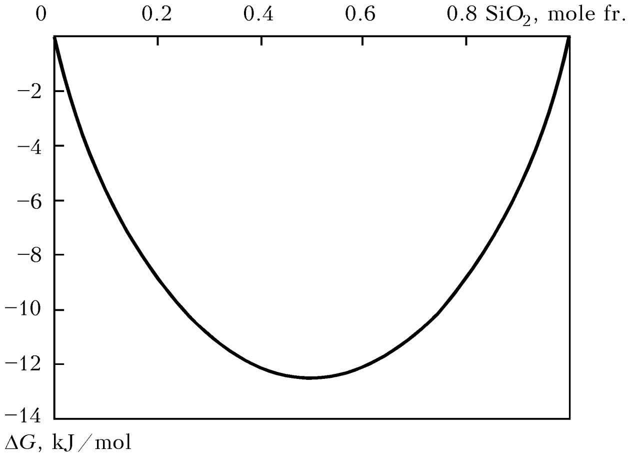

Figure 4. Gibbs mixing energy of Al_2O_3–SiO_2 system melts at 2160 K

quite valid, either, as they demonstrate considerable temperature dependencies in a narrow temperature range. Therefore, we believe that the data obtained by us provide the most adequate insight into the actual nature of liquid state interaction (at small overheating above the liquidus line). The advantage of our method consists in that with the availability of our reliable experimental data on phase equilibria, it always allows obtaining component activities, close to those found by accurate experimental methods.

We calculated Gibbs mixing energy from the obtained component activities (Figure 4).

As one would expect, it is characterized by small absolute values. Nonetheless, at addition of alkali-earth metal oxides and fluorides, a strong interaction of the latter both with SiO_2 and with Al_2O_3 can be observed, that follows from the data for melts of $CaO–SiO_2(Al_2O_3)$ binary systems [25]. Therefore, the influence of the considered system on the nature of interaction in complex multicomponent fluxes can be significant.

Thus, presence of strong interaction due to these factors should be taken into account at investigation and application of the actual oxide-fluoride melts.

Performed analysis of thermodynamic properties of $Al_2O_3–SiO_2$ system melts led to the assumption that addition of thermodynamically stable chemical compounds based on silicon and aluminium oxides to multicomponent slag melts, will allow lowering the oxidizing ability of the slag melt relative to molten metal, reducing the alloying element losses in welding and ESR and preventing the occurrence of silicon-reduction process in the metal of weld and ingot, which is undesirable in terms of metallurgy, welding and ESR of high-strength steels.

To check this assumption, EDS method was used to study oxygen activities in melts of agglomerated fluxes of $MgO–Al_2O_3–SiO_2–CaF_3–TiO_2$ system. Slags had approximately the same composition and differed just by the method of addition of silicon and aluminium oxides to agglomerated flux charge. In one case alumina and quartz sand were added, and in the second case this was disthen-sillimanite concentrate, in which these oxides are bound in Al_2SiO_5 complex compound.

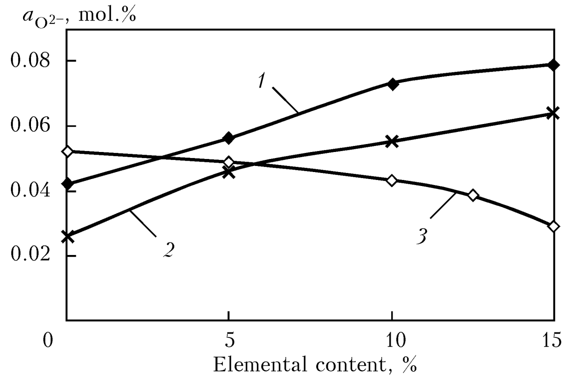

Figure 5. Dependence of oxygen activity in slag melt of $MgO–Al_2O_3–SiO_2–TiO_2$ system on the content of quartz sand (*1*), alumina (*2*) and disthen-sillimanite concentrate Al_2SiO_5 (*3*) in agglomerated flux charge

Figure 5 shows the dependence of oxygen activity in slag melts on these components content in slag melt charge. It is established that addition of alumina and quartz sand leads to increase of oxygen activity in the slag melt. At their replacement by disthen-sillimanite concentrate oxygen activity in the slag melt drops noticeably. This is attributable to high thermal stability and insignificant dissociation of Al_2SiO_5 compound and to melt dilution by an inert substance.

We also determined [Si], [Mn] content in the deposited metal in submerged-arc welding with fluxes based on disthen-sillimanite concentrate (701), as well as those based on quartz sand and alumina (705) (Figure 6).

Figure 6 shows that replacement of quartz sand and alumina by thermodynamically stable disthen-sillimanite concentrate leads to lowering of manganese losses in the weld metal, and es-

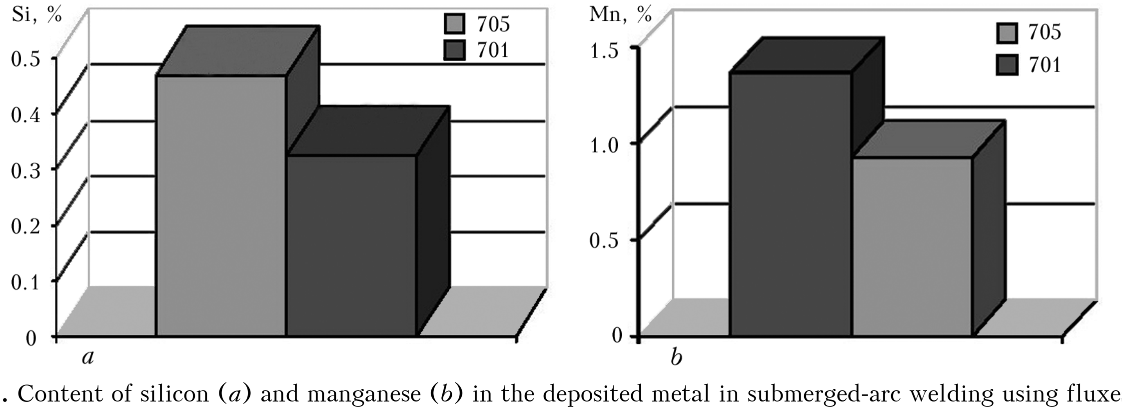

Figure 6. Content of silicon (*a*) and manganese (*b*) in the deposited metal in submerged-arc welding using fluxes based on disthen-sillimanite concentrate (701), as well as those based on quartz sand and alumina (705), with application of Sv-08G1NMA wire

sential prevention of running of silicon-reduction process.

Thus, the attractiveness of disthen-sillimanite concentrate application in manufacture of agglomerated welding fluxes is obvious.

Conclusions

1. Performed analysis of published data on phase equilibria and thermodynamic properties of Al_2O_3–SiO_2 system alloys revealed that the constitutional diagram is correct, and component activities of these alloys are characterized by large scatter.

2. Coordinates of liquidus line of Al_2O_3–SiO_2 system constitutional diagram, determined by different authors, were used to calculate $a_{Al_2O_3}$ activities at $0.7 < x_{Al_2O_3} < 1$. It is established that they start manifesting small negative deviations from ideal solutions in eutectic melt ($x_{Al_2O_3} = 0.74$).

3. Proceeding from $a_{Al_2O_3}$ values, calculated by us, integration of Gibbs–Dugem equation was used to evaluate silicon oxide activities. It is established that they demonstrate slight negative deviations from ideal solutions.

4. Influence of Al_2O_3–SiO_2 system melts on the nature of interaction in multicomponent solutions can be significant.

5. Addition of thermally-stable chemical compounds (for instance, sillimanite) to multicomponent slag melts leads to lowering of their oxidizing ability. Replacement of quartz sand and alumina by disthen-sillimanite concentrate in agglomerated flux charge leads to lowering of thermodynamic activity of oxygen in the slag melt, slows down the silicon-reduction process and reduces manganese losses in welding.

1. Zajtsev, A.I., Mogutnov, B.M., Shakhpazov, E.Kh. (2008) *Physical chemistry of metallurgical slags*. Moscow: Interkontakt Nauka.
2. Shepherd, E.S., Rankin, G.A., Wright, F.E. (1909) The binary systems of alumina with silica, lime and magnesia. *Am. J. Sci.*, **28**, 293–298.
3. Bowen, N.L., Greig, J.W. (1924) The system alumina-silica. *J. Am. Ceram. Soc.*, **7**, 238–254.
4. Bowen, N.L., Greig, J.W., Zies, E.G. (1924) Mullite, a silicate of alumina. *J. of the Washington Academy of Sci.*, **14**, 183–191.
5. Chaudhuri, S.P. (1987) Melting/decomposition of mullite: Incongruent or congruent? Pt I: Phase equilibria of the system aluma-silica. *Ceram. Int.*, 13(**3**), 167–175.
6. Chaudhuri, S.P. (1987) Melting/decomposition of mullite: Incongruent or congruent? Pt II: Responsible factors for dual nature of mullite. *Ibid.*, 13(**3**), 177–181.
7. Gao, Z. (1981) Review of studies and controversy on the phase diagram of the alumina-silica system. *Ibid.*, 9(**2**), 197–217.
8. Mueller-Hesse, H. (1963) The development of investigations and present-day knowledge of the system Al_2O_3–SiO_2. *Ber. Deut. Keram. Ges.*, 40(**5**), 281–285.
9. Pask, J.A. (1990) Critical review of phase equilibria in the alumina-silica system. *Ceram. Transact.*, **6**, 1–13.
10. Roy, R. (1990) The alumina-silica phase diagram: Metastability and order-disorder. *Ibid.*, **45–50**, 1–132.
11. Jantzen, C.M., Schwahn, D., Schelten, J. et al. (1981) The silica alumina system. Pt 1: Later stage spinodal decomposition and metastable immiscibility. *Phys. Chem. Glasses*, 22(**5**), 122–137.
12. Shornikov, S.I., Archakov, I.Yu. (2000) Mass-spectrometric study of processes of evaporation and phase equilibria in Al_2O_3–SiO_2 system. *Zhurnal Phys. Khimii*, 74(**5**), 775–782.
13. Aksay, I.A., Pask, J.A. (1975) Stable and metastable equilibriums in the system silica-alumina. *J. Am. Ceram. Soc.*, 58(**11/12**), 507–512.
14. Staronka, A., Pham, H., Rolin, M. (1968) Cooling curve study on the silica-alumina system. *Revue Int. des Hautes Temp. et des Refractaires*, 5(**2**), 111–115.
15. Aramaki, S., Roy, R. (1962) Revised phase diagram for the system Al_2O_3–SiO_2. *Ibid.*, **45**, 229–242.
16. Zajtsev, A.I., Litvina, A.D., Mogutnov, B.M. (1995) Thermodynamical properties of mullite $3Al_2O_3{\cdot}2SiO_2$. *Neorgan. Materialy*, 31(**6**), 768–772.
17. Shornikov, S.I., Stolyarova, V.L., Shultz, M.M. (1994) High temperature mass spectrometric study of $3Al_2O_3{\cdot}2SiO_2$. *Rapid Commun. Mass Spectrom.*, 8(**6**), 478–480.
18. Dhima, A., Stafa, B., Allibert, M. (1986) Activity measurements in steelmaking-related oxide melts by differential mass spectrometry. *High Temperature Sci.*, 21(**3**), 143–159.
19. Shornikov, S.I., Archakov, I.Yu., Chemekova, T.Yu. (2000) Mass spectrometric study of thermodynamical properties of Al_2O_3–SiO_2 melts. *Zhurnal Phys. Khimii*, 74(**5**), 783–788.
20. Bjorkvall, J., Stolyarova, V.L. (2001) A mass spectrometric study of Al_2O_3–SiO_2 melts using a Knudsen cell. *Rapid Commun. Mass Spectrom.*, 15(**10**), 836–842.
21. Bondar, V.V., Lopatin, S.I., Stolyarova, V.L. (2005) Thermodynamical properties of Al_2O_3–SiO_2 system at high temperatures. *Neorgan. Materialy*, 41(**4**), 362–369.
22. Mao, H., Seleby, M., Sundman, B. (2005) Phase equilibria and thermodynamics in the Al_2O_3–SiO_2 system modeling of mullite and liquid. *J. Am. Ceram. Soc.*, 88(**9**), 2544–2551.
23. Jak, E., Hayes, P.C., Pelton, A.D. et al. (2009) Thermodynamic modeling of the Al_2O_3–CaO–FeO–Fe_2O_3–PbO–SiO_2–ZnO system with addition of K and Na with metallurgical applications. In: *Proc. of 8th Int. Conf. on Molten Slags, Fluxes and Salts*, 473–490. Santiago: Geramin.
24. Sudavtsova, V.S., Makara, V.A., Kudin, V.G. (2005) *Thermodynamics of metallurgical and welding melts*. Pt 3: Alloys based on nickel and tin, methods of modeling and prediction of thermodynamic properties. Kiev: Logos.
25. Goncharov, I.A., Galinich, V.I., Mishchenko, D.D. et al. (2014) Prediction of thermodynamic properties of melts of Al_2O_3–SiO_2 system. *The Paton Welding J.*, **4**, 26–29.

Received 30.10.2014